Received: 27 June 2019 | Revised: 24 September 2019 | Accepted: 15 October 2019

DOI: 10.1002/pip.3214

EU PVSEC PAPER

WILEY PROGRESS IN PHOTOVOLTAICS

Photovoltaic operation in the lower atmosphere and at the surface of Venus

Jonathan Grandidier[1,3] | Alexander P. Kirk[2] | Phillip Jahelka[3] | Margaret A. Stevens[4] | Pawan K. Gogna[1] | David Crisp[1] | Mark L. Osowski[2] | Thomas E. Vandervelde[4] | Harry A. Atwater[3] | James A. Cutts[1]

[1] Jet Propulsion Laboratory, California Institute of Technology, Pasadena, CA 91109, USA

[2] MicroLink Devices Inc., Niles, IL 60714, USA

[3] Thomas J. Watson Laboratory of Applied Physics, California Institute of Technology, Pasadena, CA 91125, USA

[4] Department of Electrical Engineering, Tufts University, Medford, MA 02155, USA

Correspondence
Jonathan Grandidier, Jet Propulsion Laboratory, California Institute of Technology, Pasadena, CA 91109, USA.
Email: jonathan.grandidier@jpl.nasa.gov

Funding information
National Aeronautics and Space Administration, Grant/Award Numbers: ROSES16 HOTTech Program, Space Technology Research Fellowship NNX15AQ79H and NNX15AQ79H; National Science Foundation, Grant/Award Number: Award no. 1541959

Abstract

Low-intensity high-temperature (LIHT) solar cells are needed for extended photovoltaic power generation in both the lower atmosphere as well as at the surface of Venus. Double-junction GaInP/GaAs solar cells that may be able to operate and survive, with suitable encapsulation, for several weeks on the 465°C Venus surface have been developed. These solar cells have been optimized for operation under the Venus solar spectrum, which is different from that of the Earth.

KEYWORDS

high-temperature photovoltaics, multi-junction solar cells, Venus exploration missions

1 | INTRODUCTION

The highest-priority science objectives, as defined by the Venus Exploration Analysis Group (VEXAG),[1] for the next generation of Venus exploration missions are to understand atmospheric formation, evolution, and climate history on Venus; to determine the evolution of the surface and interior of Venus; and to understand the complex nature of interior-surface-atmosphere interactions over time, including whether liquid water was ever present.

Venus exploration mission concepts under consideration include: variable altitude aerial platforms, near-surface aerial platforms with regional mobility, long-duration surface missions, and Venus sample return missions. Such missions are challenging to execute due to the harsh Venus aerial and surface environmental conditions such as high temperature, high pressure, and presence of corrosive chemicals.

To meet the potential Venus exploration objectives in the next Decadal Survey of planetary science, VEXAG has recommended that NASA develop the required critical spacecraft systems, subsystems, and payload instruments that could survive and operate in the harsh aerial and surface environment of Venus for long duration. Advanced high-temperature power systems are one of the key subsystem technologies identified by VEXAG for development and technology maturation. Power technology options for Venus missions include radioisotope power systems (RPS), batteries, wind energy, and photovoltaic power systems. Photovoltaics may have the advantage to produce energy for long duration at a limited cost. Previous work on high-temperature solar cells that could survive at Venus was done.[2-4] Figure 1 shows a concept for a photovoltaic-powered lander on the surface of Venus. Here, we describe the development of double-junction (2J) GaInP/GaAs solar cells that can operate and survive for an extended period of time in the lowest ~21 km of the atmosphere and at the surface of Venus. For example, the Long-Lived In-Situ Solar System Explorer (LLISSE) lander has a target of 2 months of operation at the surface of Venus.[5] An optimized solar cell for these conditions is presented. Current–voltage (*I*–*V*) and external quantum efficiency (EQE) measurements weighted by the Venus solar

FIGURE 1 Artist's concept of a photovoltaic-powered lander at the surface of Venus. Artwork by Justin Van Genderen. [Colour figure can be viewed at wileyonlinelibrary.com]

spectrum under lower atmospheric and surface conditions are shown. Lifetime testing results of the 2J cell performance before and after heating for up to seven weeks at 465°C, which corresponds to the surface temperature of Venus, are presented. Finally, solar cell modeling is used to evaluate the performance of various solar cell designs at various altitudes on Venus.

2 | SOLAR INTENSITY AT VENUS

The solar spectrum in the Venus atmosphere is different from that on Earth and varies significantly with altitude. Absorption and scattering by the atmosphere and thick cloud structure[6] reduces the intensity from ~2622 W/m^2 above the atmosphere to < 100 W/m^2 at the surface. This was measured by the two Soviet descent probes, Venera 11[7] and Venera 13,[8] which recorded the spectrally dependent downward solar radiation at altitudes between 62 km and the surface. Figure 2 shows the Venus atmospheric structure with three layers of clouds. The solar flux was calculated based on the Venera 11[7] measurements (solar zenith angle 17°). The downward solar flux is a strong function of both solar zenith angle and cloud opacity. The pressure at the surface of Venus is 90 bars. The atmosphere is composed of 96% carbon dioxide (CO_2) and 3.5% nitrogen (N_2). It also includes traces of sulfur dioxide (SO_2, 150 ppm), water vapor (H_2O, 30 ppm), carbonyl sulfide (COS, 4 ppm), and hydrogen chloride (HCl, 0.5 ppm).[9]

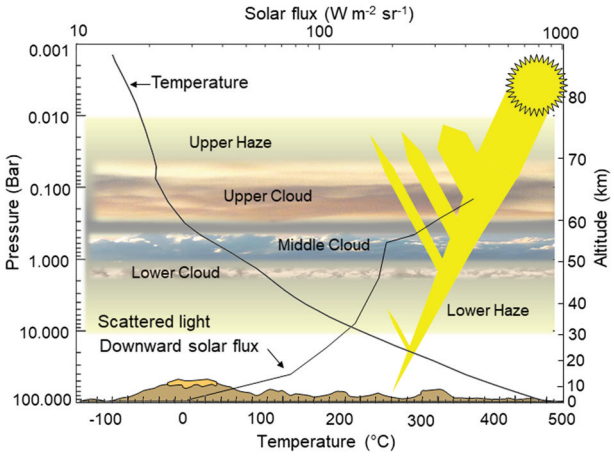

FIGURE 2 Schematic of the Venus atmosphere. Temperature, pressure, and solar flux are represented. Solar flux was measured by Venera 11 (solar zenith angle 17°). [Colour figure can be viewed at wileyonlinelibrary.com]

3 | VENUS-OPTIMIZED SOLAR CELL

Data from Venera 11 were used to optimize the 2J models, as the measurements were taken near noon local time and are, therefore, closer to the highest solar intensity values that can be expected. Using the validated modeling method described in Section 6, we explored and optimized possible solar cell designs for operation on Venus. We first investigated the altitude performance of a standard 2J GaInP/GaAs MicroLink Devices solar cell as a function of GaInP subcell thickness. Additional details on the solar cell structure are given in the reference.[4] Results are plotted in Figure 3a, where the color represents the generated electrical power, and the black line is the optimal GaInP thickness for each altitude. Modeling shows that a 2J solar cell optimized for an altitude of 21 km on Venus, where the temperature is 300°C, would generate 41.5 W/m^2 and have a GaInP subcell thickness of 200 nm. Although the solar spectrum varies significantly within the atmosphere of Venus, the optimum solar cell structure has a GaInP subcell thickness of 200 nm for altitudes between 10 km and 50 km. This is due to other environmental characteristics such as the temperature variation that compensates for the solar spectrum variation. Below a 10 km altitude, the flux of high-energy photons (λ < 0.7 μm) rapidly decreases, which necessitates thickening the GaInP subcell to maintain current matching between it and the GaAs subcell. Figure 3b shows a simplified schematic of a standard MicroLink Devices solar cell that is optimized for Earth AM0 solar illumination. Figure 3c shows a schematic of a modified GaInP/GaAs solar cell design fabricated for the Venus atmosphere at an altitude of 21 km and a temperature of 300°C.

The fabricated design incorporates a thin GaInP subcell with a thickness of 220 nm (which is close to the 200 nm calculated optimum). The above layer structure was grown by metal-organic chemical vapor deposition (MOCVD) on p-doped GaAs substrates miscut 6 degrees toward the (111)A plane and subsequently fabricated into solar cell devices.

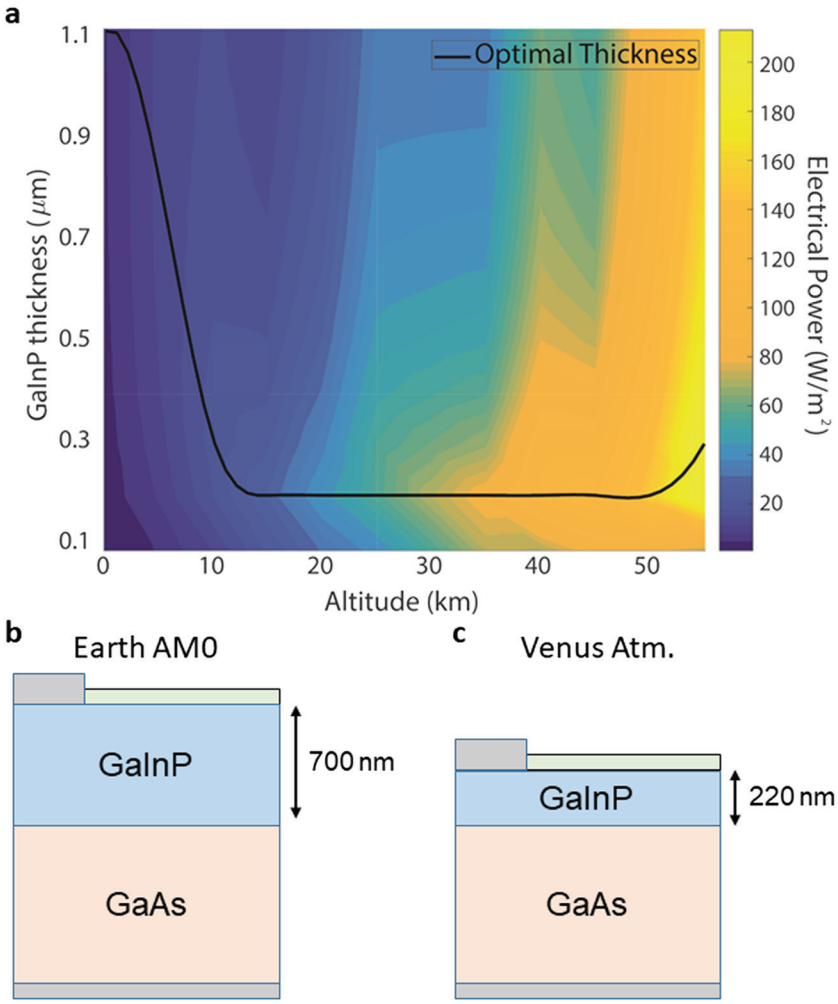

FIGURE 3 (a) Modeled electrical power output for a double-junction GaInP/GaAs solar cell as a function of altitude and top junction thickness. Calculated result incorporates spectrum and temperature as a function of altitude. The black line shows the optimal thickness at a given altitude. (b) Earth AM0-optimized solar cell. (c) Modified solar cell that was fabricated for operation in the Venus atmosphere at 21 km and 300°C. [Colour figure can be viewed at wileyonlinelibrary.com]

The EQE of a fabricated Venus solar cell, Figure 3c, was measured at 300°C and weighted by the 21 km Venus solar spectrum based on Venera 11 measurements.[7] Figure 4 shows the spectral current density.[10,11] Both junctions are nearly current balanced with the top subcell being slightly current limiting. With a solar intensity at 21 km of 128.3 W/m^2/sr,[4] the current density of the GaInP subcell is 2.21 mA/cm^2, whereas the current density of the GaAs subcell is 2.29 mA/cm^2. This result validates our design for a mid-altitude Venus solar cell. Accounting for the angular acceptance of the solar cell[12] and isotropic downward solar flux as described in,[4] we can estimate from the current-limiting top subcell a short circuit current J_{sc} = 4.72 mA/cm^2. Using our model described in Section 6, we calculated an open circuit voltage V_{oc} = 1.10 V, fill factor *FF* = 0.68, and estimated power density P = 35.3 W/m^2.

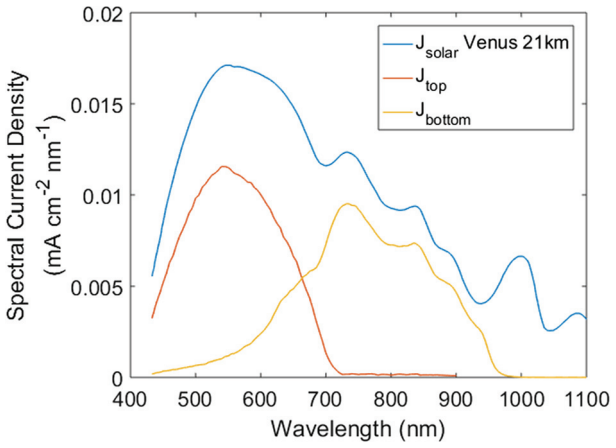

FIGURE 4 Balanced spectral current density for a 21 km/300°C Venus-optimized solar cell using the measured 300°C EQE weighted by the 21 km Venus solar spectrum. [Colour figure can be viewed at wileyonlinelibrary.com]

4 | VENUS SURFACE MEASUREMENT

High-temperature *I*–*V* measurements were performed on the mid-altitude (~21 km) Venus atmosphere–optimized solar cell. For these measurements, an AM0 solar simulator was used to illuminate a solar cell while heated. The solar cell was mechanically held on a steel plate on which temperature was measured. Figure 5a shows the *I*-*V* measurements of a solar cell between 25°C and 465°C while illuminated under 1-Sun AM0 (~1367 W/m^2). As expected, an increase in temperature results in a decrease in V_{oc}[13,14] from 2.27 V at 25°C to 0.72 V at 465°C. As shown in Figure 5a, J_{sc} remains stable at ~14 mA/cm^2 up to 200°C and then increases to 16.8 mA/cm^2 at 465°C. The *FF* decreases

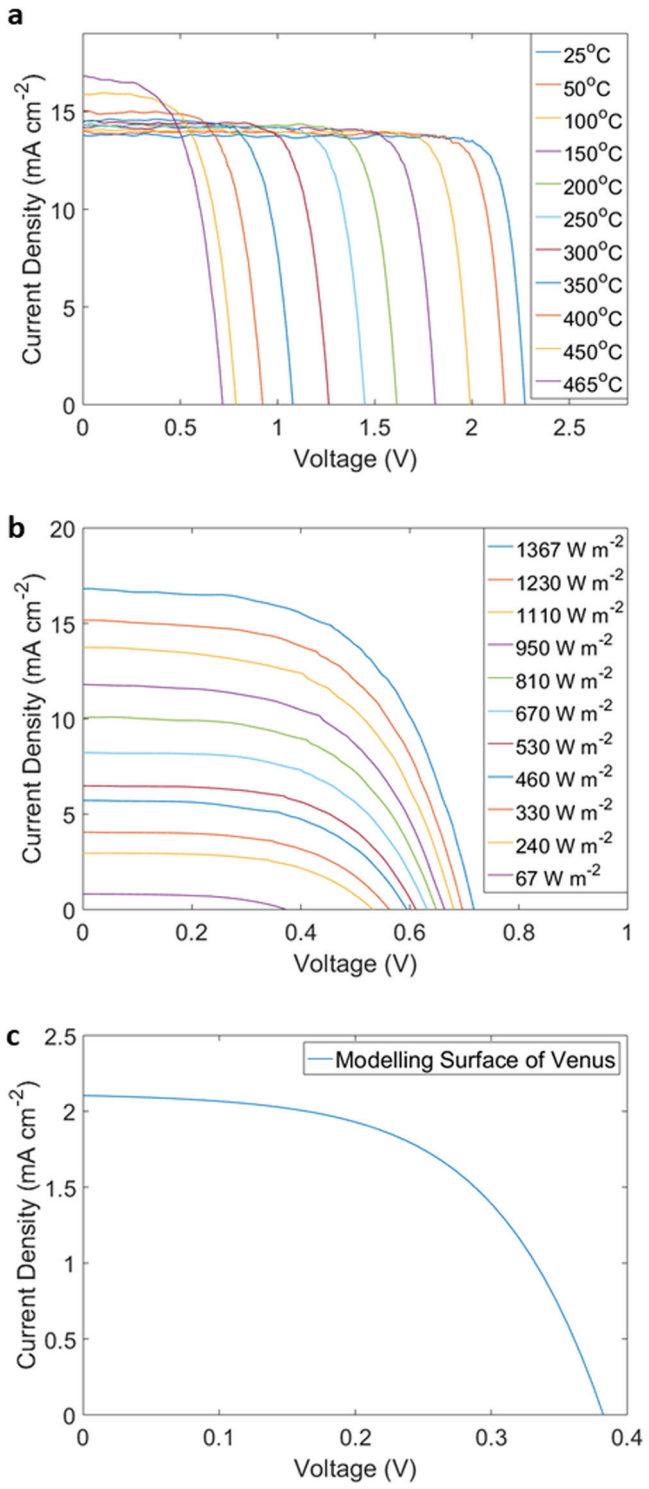

FIGURE 5 (a) Variable-temperature *I*–*V* measurements of a GaInP/GaAs 2J solar cell between 25 and 465°C (Venus surface temperature) using an AM0 solar simulator. (b) Light *I*-*V* measurements of a solar cell heated at 465°C while illuminated between 1367 W/m^2 (1-Sun AM0 spectrum) and 67 W/m^2 (Venus surface illumination intensity). (c) Modeled light *I*-*V* curve of a solar cell optimized for Venus surface conditions under Venus surface temperature solar spectrum. [Colour figure can be viewed at wileyonlinelibrary.com]

from 0.86 to 0.59 between 25°C and 465°C. Figure 5b presents *I*–*V* measurements between 1-Sun AM0 conditions and 67 W/m^2. This low illumination intensity is close to what the solar cell would be exposed to at the surface of Venus, accounting for diffused light and incident angle.[15,16] To achieve lower light illumination, the solar simulator power was decreased linearly with short circuit current and neutral density filters were used. Under conditions close to the surface of Venus, except for the spectrum, 465°C and 67 W/m^2, the measured solar cell characteristics were: V_{oc} = 369 mV, J_{sc} = 0.83 mA/cm^2, *FF* = 0.54, power density *P* = 1.6 W/m^2, and power conversion efficiency η = 2.45%. The efficiency was limited because the subcell current balancing was optimized for a different temperature and spectrum than the one used for the test. Although preliminary modeling had suggested the solar cell would not be functional under Venus surface conditions, the solar cell was actually still functional under these extreme conditions even though it was designed for more benign mid-altitude, 21 km and 300°C, conditions.

Modeling was used to estimate the characteristics of an optimized solar cell under Venus surface conditions. The model assumed a temperature of 465°C, a solar intensity of 67 W/m^2, and the solar spectrum at the surface of Venus as it was measured by Venera 11. Figure 5c shows the modeled *I*–*V* curve of the Venus surface–optimized solar cell. This solar cell is a modified 2J GaInP/GaAs device with thicker window and back surface field (BSF) layers, see Figure 10 c of Section 6. Characteristics are V_{oc} = 380 mV, J_{sc} = 2.1 mA/cm^2, *FF* = 0.54 for an overall efficiency of 6.4%, and a generated power of 4.3 W/m^2. As a comparison, this is similar to the power generated by a high-efficiency solar cell[17] at Saturn,[18] and the very low power generation capability presents a very high challenge. These values only account for the downward flux at the surface of Venus. Because upward (scattered) solar flux is important in the Venus atmosphere,[19] power generation could be increased by taking advantage of it.

5 | LIFETIME TESTING

Heat-exposure tests were performed on the GaInP/GaAs 2J solar cells with temperatures at 465°C. The cells were fabricated with an improved high-temperature metal stack consisting of a platinum (Pt) based barrier metal and a silver (Ag) conducting layer. The *I*–*V* behavior was measured at 25°C under simulated AM0 1-Sun illumination before and after heating on a hot plate and is shown in Figure 6. The high-temperature soak was performed for up to seven weeks in a high-vacuum chamber (10^{-7} torr), which is different from being subjected to a Venus surface pressure of 90 bars. The effect on the semiconductor bandgaps is not significant at this pressure.[20] Prior to heating, the solar cell efficiency measured under the 1-Sun AM0 solar spectrum was ~23%. Solar cells were first heated for one week, two weeks, three weeks, four weeks, and seven weeks at 465°C. While some cells degraded after four weeks of exposure, the best performing cell did not degrade until after seven weeks of exposure at 465°C. After four weeks of exposure at 465°C, some cells experienced a higher series resistance and no reduction in V_{oc}. Visible (red)

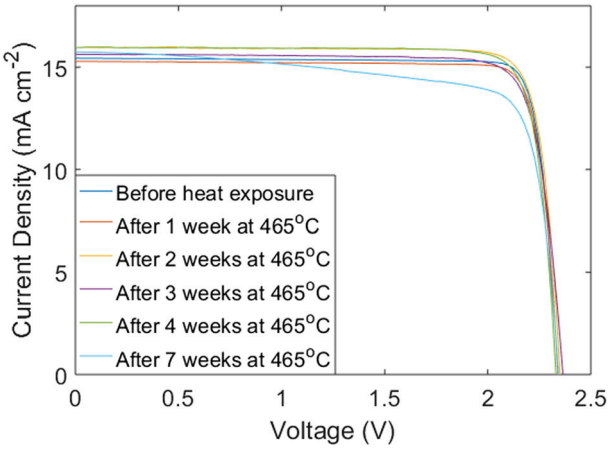

FIGURE 6 *I–V* response (AM0 spectrum) of a GaInP/GaAs 2J solar cell with a high-temperature grid metal and an $Al_2O_3/TiO_x/Al_2O_3$ antireflective coating (ARC) before and after heating on a 465°C hot plate for up to seven weeks in a high-vacuum chamber. [Colour figure can be viewed at wileyonlinelibrary.com]

electroluminescence (EL) from the GaInP subcell, centralized at the wider busbar contact, but dim under the narrower gridline contact (not shown), may indicate the onset of increased series resistance after four weeks of heat soaking. This is possibly resulting from oxidation of the grid metal, formation of resistive material at the metal-semiconductor interface, or oxidation of the thin AlInP window–GaInP emitter region of the solar cells; noting that oxidation of the AlInP-GaInP interface region could cause both series resistance and suboptimal passivation. Despite the fill factor degrading after seven weeks of heating, the solar cell yielded a post-heat exposure efficiency of 20.5% under the 1-Sun AM0 spectrum at 25°C. These findings represent a significant improvement from previous measurements.[4]

To investigate the origins of the electrical degradation, scanning electron microscopy (SEM) and scanning transmission electron microscopy (STEM) were used to image the Ag contact bars and the surrounding area. SEM images and cross-sectional STEM samples were created with a FEI Helios dual electron and focused ion beam (FIB) microscope equipped with an energy dispersive x-ray spectroscopy (EDS) detector. STEM images were collected using a JEOL 200F ARM atomic resolution microscope. A high-angle annular dark field (HAADF) detector was used to highlight changes in contrast due to atomic size, and EDS was used to identify changes in composition.

Two solar cells were investigated: one that was not heat-treated and had 1-Sun AM0 efficiency of 23%, and one that was subjected to 4 weeks of heat soaking at 465°C, which caused the 1-Sun AM0 efficiency to degrade to 17% through a reduction of the fill factor. Although lifetime testing was done in a high-vacuum chamber, the onset of noticeable series and shunt resistance after 4 weeks of heat soaking at 465°C may have been caused by slow but eventual oxidation of the Ag grid metal, the metal-semiconductor interface, or the AlInP window–GaInP emitter region. Additionally, Ag is also known to diffuse quickly in both GaAs and InP, where even mild annealing can result in roughly uniform 1×10^{16} cm^{-3} Ag concentration throughout the whole wafer.[21,22] It is suspected the Ag is interstitial and forms a deep donor that, while not recombination active, could degrade the mobility and compensate *p*-type doping. Both of these effects may increase series resistance and decrease the fill factor as observed in the degraded samples annealed for four weeks.

Figure 7 shows top-view SEM images of the metal contact bars on the heated cell (a) and the unheated cell (b). The solar cell that suffered from degradation after heating at 465°C for 4 weeks (a) looks identical to a solar cell that was not subjected to heat treatment (b) even though the electrical performance suffered. Cross-sectional STEM imaging directly underneath the metal contact (not shown) reveals metal divots extending from the metal into the thick GaAs contact layer underneath. This is expected for thermal treatment of metal contacts and typically decreases contact resistance,[23] which, in theory, should improve the device performance. Therefore, to look for the cause of the electrical degradation, we investigated the region of the solar cell around the metal contacts.

Figure 7c shows an increased magnification SEM image of the area surrounding the metal contacts on the heat-treated solar cell. Large droplets with a diameter of ~200 nm extend from next to the metal contact to as far as 5 μm away from it. These droplets are also found in the unheated solar cell and can be seen in Figure 7b. The EDS map shown in Figure 7d reveals the droplets to contain Ag as indicated by the green signal. Ag is one of the primary components of the metal stack used in the grid bars; therefore, it is likely these metal droplets originate from the metal grid bars. However, it is presently not known why they are present on both the heated and the unheated cells.

Cross-section STEM of regions of the solar cell directly next to the contacts shows that the Ag droplets can form divots that extend into the III-V semiconducting region. Directly next to the metal contact, the underlying GaInP solar cell is protected from the metal by a thin layer of the GaAs top contact layer; however, EDS mapping shows this layer only extends 1 μm on each side of the metal contact. Figure 8 shows a cross-sectional STEM image of the top GaInP solar cell 2–3 μm away from the metal contact bar and away from the protection of the GaAs contact layer. The Ag droplets are seen to spill over or form divots that extend into the top GaInP subcell. In Figure 8, the divots extend down to the GaInP *p-n* junction, which could lead to degradation of the shunt resistance by shorting the junction. While we found Ag droplets leading to contamination and divots in both solar cells (heated and unheated), it appears to be far more prevalent in the heated cell, Figure 8a. Additionally, it is also possible that these metal droplets and their extended divots could lead to the diffusion of smaller Ag particles into the top subcell with size less than the resolution of the STEM. As previously mentioned, this could be a source of fill factor degradation. To mitigate this issue, future high-temperature PV cells could employ a thin GaAs contact layer that extends at least 5 μm to each side of the top contact to protect the underlying solar cell.

Additional contributions to series resistance degradation could involve oxidation of the grid metal, formation of resistive material at the metal-semiconductor interface, or oxidation of the thin AlInP window–GaInP emitter region of the solar cells. Oxidation of the AlInP-GaInP interface region could cause both series resistance and

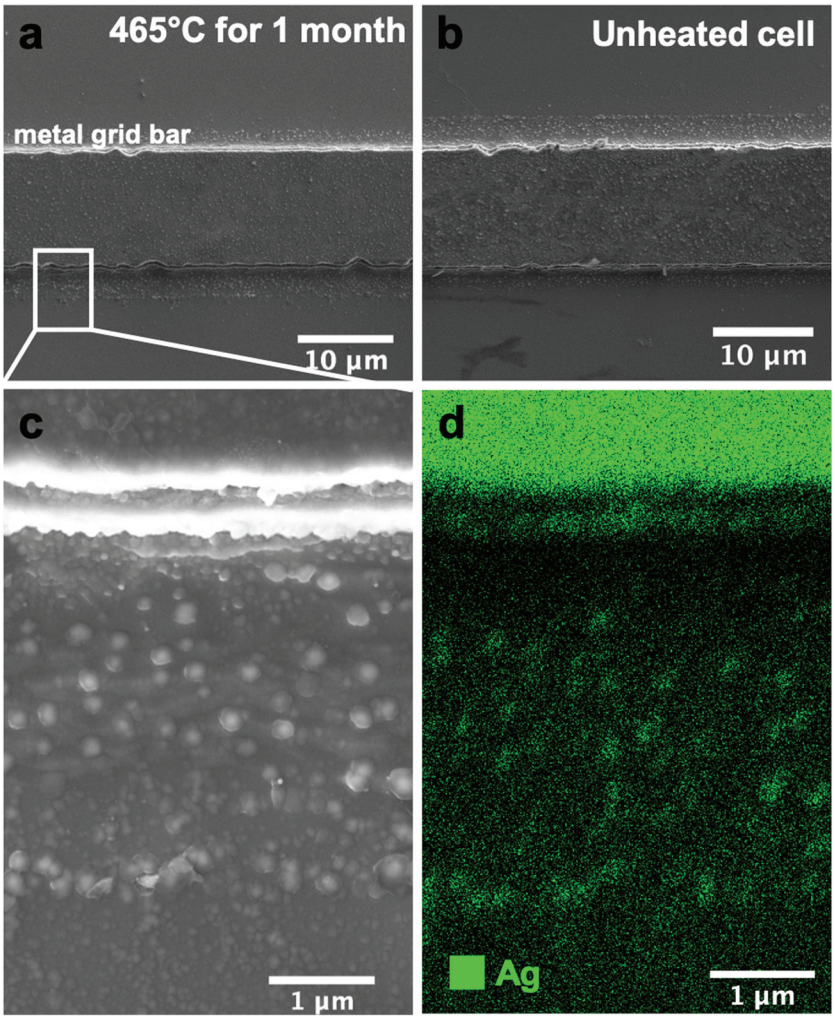

FIGURE 7 (a) Top-view SEM image of metal grid bars on solar cell heated to 465°C for 1 month. (b) Image of solar cell with no heat treatment. (c) Increased magnification image of droplets found next to contact. (d) EDS image showing Ag signal. [Colour figure can be viewed at wileyonlinelibrary.com]

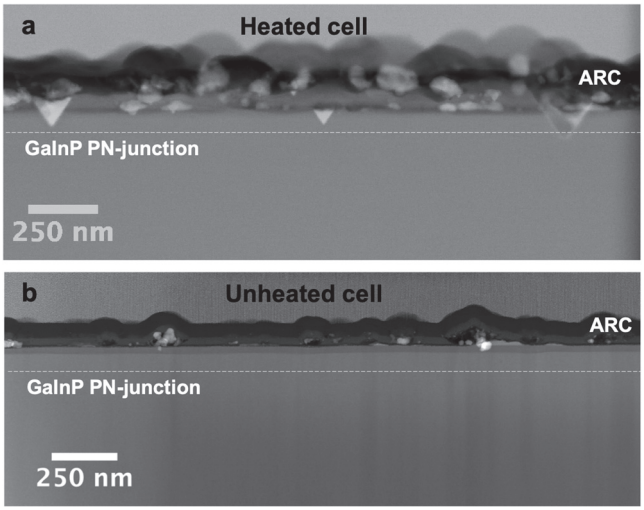

FIGURE 8 (a) Cross-sectional STEM view of the heated solar cell looking at the interface between the ARC and the GaInP cell. Ag droplets form divots that extend into the III-V layer. Some are deep enough to reach the GaInP *p-n* junction. (b) Cross-sectional STEM view of the unheated solar cell. While the Ag droplets lead to some contamination and divots in the III-V layer, it is less severe than in the heated solar cell.

suboptimal passivation. While significant oxidation of these layers was not found via EDS measurements, other techniques such as x-ray photoelectron spectroscopy (XPS) combined with depth-profiling should be employed in future encapsulation studies to ensure no unintended oxidation is occurring.

We assessed here the effect of high temperature on the solar cell. An understanding of material reactions in Venus relevant atmospheric conditions is needed to enable future Venus missions.[24] In order to survive the Venus corrosive environment, we expect the solar cells will need a suitable encapsulation. This type of encapsulation is currently under development[25] and would need to be adapted for a solar cell with a transparent facet.

6 | SOLAR CELL MODELING

Modeling was used to evaluate the performance of several solar cell designs at various altitudes on Venus. We first refined our semiconductor device physics models to reproduce the measured temperature dependence of EQE and V_{oc} of the Venus-optimized solar cell depicted in Figure 3c. Once our models reproduced measured results, we explored and optimized solar cell designs for operation on Venus.

Satisfactorily reproducing the measured EQE curves required consideration of the temperature dependence of both the material bandgaps and Urbach tails. The Urbach tail is an exponentially decreasing sub-bandgap tail in a material's absorption spectrum. Despite its ubiquity and thorough characterization, a theoretical understanding of its origin remains elusive. To implement the Urbach tail in the optical portion of our simulations, we define the absorption coefficient, α, to be

$$\alpha(E) = \begin{cases} \alpha_{exp},\ \alpha > 8000/cm \\ (8000/cm)e^{(E-E_g)/E_0},\ \text{otherwise} \end{cases},$$

where E is the photon energy, α_{exp} is the above-gap temperature- and energy-dependent absorption coefficient, E_g is the bandgap, and E_0 is the temperature-dependent Urbach parameter that controls the rate of the exponential decay. $\alpha = 8000/cm$ is chosen as the boundary between usual absorption and Urbach absorption to follow Johnson and Tiedje, who characterized the temperature-dependent Urbach tail of GaAs.[26] Johnson and Tiedje also discovered a linear relationship between E_0 and the temperature-dependent bandgap narrowing for GaAs. By assuming the same proportionality for other materials, we were able to predict the Urbach tail for all materials in the device. In Figure 9a, we demonstrate the importance of including the Urbach tail by comparing the GaAs subcell band-edge EQE at 300°C of two experimentally measured cells, one by our measurements and one from literature by Steiner et al.,[27] and two simulated cells, one which includes the Urbach tail and one that does not. The simulated EQE that includes the Urbach tail falls between the two experimental EQE curves, while the simulation without the Urbach tail has a much higher energy and sharper absorption edge. Because our simulated EQE is now comparable to experimental EQE, we can faithfully model the material's optical properties as a function of temperature.

The next cell parameter we worked to reproduce was the open circuit voltage of the modified Venus solar cell (Figure 3c) as a function of temperature. Using TCAD Sentaurus's built-in recombination models, we drastically underestimate V_{oc} at high temperature, as illustrated in Figure 9b. By multiplying the built-in lifetimes by a factor with exponential temperature dependence, we could reproduce the measured V_{oc}.

Using our validated model, we explored the modification of other aspects of the design to improve the performance at the surface of Venus. In our simulations, we included diffuse illumination, and the altitude dependence of the spectrum and total power. To do so, we used the spectrum provided by Moroz et. al. and multiplied the spectrum by 0.68 to derate the ARC for diffuse illumination.[4,7,15]

In exploring the design space, we found that increasing the thickness of the window and BSF layers could dramatically increase performance at high temperature. For example, by changing the windows thickness from 25 nm to 100 nm and the BSF thickness from 25 nm to 200 nm, we could improve the power generated by a 2J GaInP/GaAs at the surface with 800 nm thick GaInP from 3.31 W/m^2 to 4.10 W/m^2, a 24% improvement. The reason for this improvement is that, at high temperatures, band-offsets are less

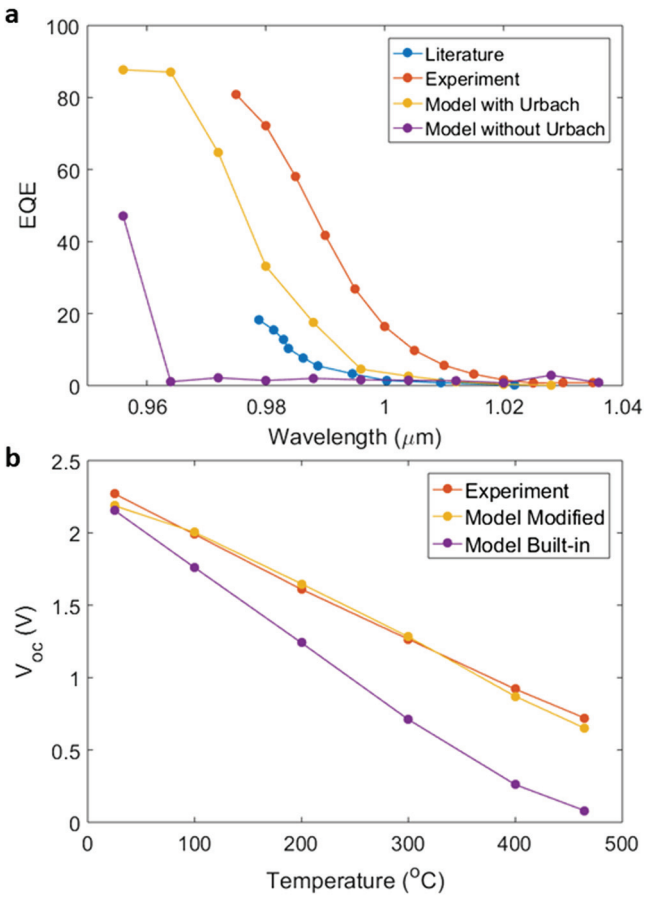

FIGURE 9 (a) Comparison of GaAs band-edge EQE at 300°C. *Literature* refers to "Steiner et al.".[27] By including the Urbach tail, our simulations fall between experimentally reported EQEs. (b) Comparison of V_{oc} of the Gen 2 cell under AM0 as a function of temperature for the measured cell and two different recombination models. We were able to successfully reproduce the observed V_{oc}. [Colour figure can be viewed at wileyonlinelibrary.com]

effective at controlling minority carriers because the minority carrier thermionic emission current over the band offset increases exponentially in temperature. By thickening the BSF and window layers, their lower bulk minority carrier conductivity takes over the role of suppressing parasitic minority carrier currents.[28]

Finally, we also considered a 3.5 μm thick, single-junction GaInP cell with either thick or thin window/BSF layers due to the lower temperature sensitivity of GaInP compared to GaAs.

From our modeling, we identified three regimes where different cells are optimal. The first is a high-altitude solar cell (Figure 10a)—a 2J cell with 200 nm GaInP and thin window/BSF (25 nm/25 nm) layers. Next is a mid-altitude solar cell (Figure 10b)—a 3.5 μm single-junction GaInP cell with thick window/BSF (100 nm/200 nm) layers. The final one is a surface/low-altitude solar cell (Figure 10c)—a 2J cell with 800 nm GaInP and thick window/BSF (100 nm/200 nm) layers. The 2J cell with 200 nm GaInP and thin window/BSF layers is best at high altitude, because the two subcells are current matched and the temperature is low enough that the GaAs subcell is producing substantial power. The dominance of the single-junction GaInP cell at

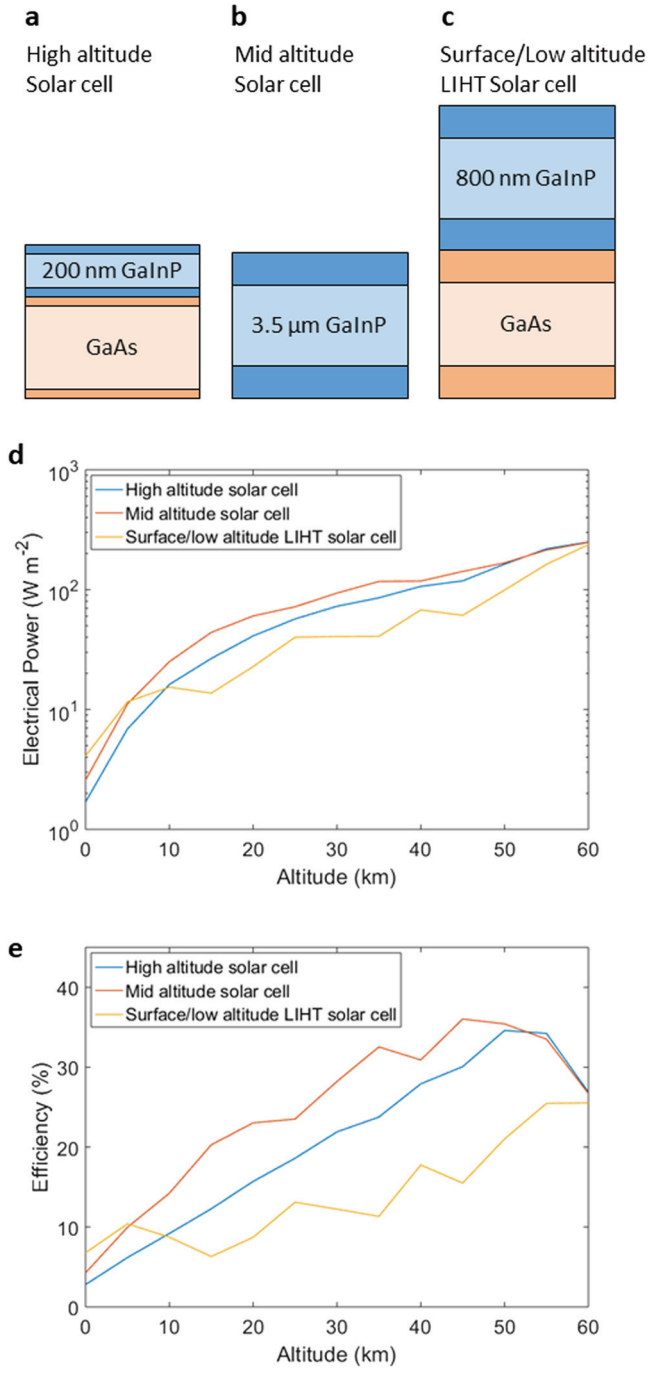

FIGURE 10 (a) High-altitude 2J solar cell design with 200 nm GaInP and thin window/BSF (25 nm/25 nm) layers. (b) Mid-altitude single-junction solar cell design with 3.5 µm GaInP and with thick window/BSF (100 nm/200 nm) layers. The cladding on each subcell represents the window/BSF layers. (c) Surface/low-altitude 2J LIHT solar cell design with 800 nm GaInP and thick window/BSF (100 nm/200 nm) layers. Modeled (d) electrical power and (e) efficiency of the different solar cell designs as a function of altitude on Venus. [Colour figure can be viewed at wileyonlinelibrary.com]

moderate altitudes is perhaps surprising because from Figure 3a we found a single GaInP thickness is optimal for a tandem over the whole mid-altitude range. However, it can be made sense of by considering that the current-matched tandem requires a very thin GaInP cell to achieve current matching by allowing high-energy photons to reach the GaAs cell. Because the performance of the GaAs subcell is rapidly decaying with temperature, it becomes parasitic compared to simply having a single GaInP cell absorbing all the light. At low altitudes, the 2J cell with thick window/BSF layers is more efficient because the temperature is high, and for the surface spectrum, a 2J with a 800 nm GaInP subcell is current matched with a GaAs bottom subcell, so the GaAs subcell is providing an additional modest amount of power without absorbing photons that are more efficiently converted by the GaInP subcell.

Figure 10d displays the power and Figure 10e displays the efficiency of each solar cell design as a function of altitude. The efficiency is what would be measured under a solar simulator with only normally incident light. The best performance we find at 21 km/300°C is 22% from the optimized single-junction GaInP cell. There are two main opportunities to improve this result. First, the anisotropic lighting[19] means we could take advantage of the upward flux and put two cells back-to-back in a bifacial configuration and significantly increase the power generated. Second, the combination of diffuse illumination and the ARC's angle dependence means we lose 30% of the light due to reflection. This could be improved by surface texturing or by using a module design that more efficiently utilizes diffuse illumination, such as a luminescent solar concentrator,[29] which is currently a topic of research.

7 | CONCLUSION

A solar cell designed for use in the atmosphere of Venus was fabricated and characterized under Venus mid-altitude and surface conditions, except for the pressure. With suitable encapsulation, GaInP/GaAs 2J solar cells may have the potential to be a solution for power generation in an extreme environment such as the surface of Venus. The analysis provided in this paper presented photovoltaic measurements of GaInP/GaAs 2J solar cells after heat soak tests at 465°C under vacuum. No appreciable degradation occurred in cell performance after four weeks of heat exposure at 465°C under vacuum. After seven weeks of exposure, solar cell performance decreased due to degradation of the fill factor. One possible cause is the slow onset of oxidation of the grid metal electrode and/or the AlInP window region of the cells. Another possible cause is metal diffusion in the active region of the cell. Finally, three solar cell designs adapted for high-altitude, mid-altitude, and surface/low-altitude conditions were proposed as a result of modeling analysis. Modeling shows that an optimized solar cell for the Venus surface could generate ~4 W/m^2.

ACKNOWLEDGEMENTS

The authors would like to thank J.A. Schwartz and A. Boca for useful inputs. The research was carried out at the Jet Propulsion Laboratory, California Institute of Technology, at MicroLink Devices Inc., at the California Institute of Technology, and at Tufts University. This work was supported by the National Aeronautics and Space Administration (NASA) through the ROSES16 HOTTech Program in the Science Mission Directorate. The work of M.A. Stevens was supported by the

NASA Space Technology Research Fellowship through Award NNX15AQ79H. This work was performed, in part, at the Center for Nanoscale Systems (CNS), a member of the National Nanotechnology Coordinated Infrastructure (NNCI) Network, which is supported by the National Science Foundation under NSF award no. 1541959. CNS is part of Harvard University.

ORCID

Jonathan Grandidier https://orcid.org/0000-0002-3384-6083
Phillip Jahelka https://orcid.org/0000-0002-1460-7933
Margaret A. Stevens https://orcid.org/0000-0002-9856-3842
David Crisp https://orcid.org/0000-0002-4573-9998
Thomas E. Vandervelde https://orcid.org/0000-0003-3696-2765
Harry A. Atwater https://orcid.org/0000-0001-9435-0201
James A. Cutts https://orcid.org/0000-0002-1765-8322

REFERENCES

1. VEXAG. Goals, Objectives, and Investigations for Venus Exploration. 2016: Jet Propulsion Laboratory.
2. Landis GA, Haag E. Analysis of Solar Cell Efficiency for Venus Atmosphere and Surface Missions, paper AIAA-2013-4028, in AIAA 11th International Energy Conversion Engineering Conference. 2013, American Institute of Aeronautics and Astronautics.
3. Perl EE, Simon J, Friedman DJ, et al. (Al)GaInP/GaAs Tandem Solar Cells for Power Conversion at Elevated Temperature and High Concentration. *IEEE J Photovolt*. 2018;8(2):640-645.
4. Grandidier J, Atwater HA, Cutts JA, et al. Low-Intensity High-Temperature (LIHT) Solar Cells for Venus Atmosphere. *IEEE J Photovolt*. 2018;8(6):1621-1626.
5. Kremic T, Hunter GW, Nero L. Long-Lived In-Situ Solar System Explorer (LLISSE). Proceedings of the Venera-D Modeling Workshop, 2017.
6. Hunten DM, Colin L, Donahue TM, Moroz VI. Venus. 1983.
7. Moroz VI, Golovin YM, Ekonomov AP, Moshkin BE, Parfent'ev NA, San'ko NF. Spectrum of the Venus day sky. *Nature*. 1980;284(5753):243-244.
8. Titov DV, Bullock MA, Crisp D, Renno NO, Taylor FW, Zasova LV. Radiation in the Atmosphere of Venus, in Exploring Venus as a Terrestrial Planet. *Am Geophys Union*. 2013;176:121-138.
9. Taylor F, Svedhem H, Head J. Venus: The Atmosphere, Climate, Surface, Interior and Near-Space Environment of an Earth-Like Planet. *Space Sci Rev*. 2018;214(1):35. https://doi.org/10.1007/s11214-018-0467-8
10. Grandidier J, Callahan DM, Munday JN, Atwater HA. Light Absorption Enhancement in Thin-Film Solar Cells Using Whispering Gallery Modes in Dielectric Nanospheres. *Adv Mater*. 2011;23(10):1272-1276.
11. Grandidier J, Callahan DM, Munday JN, Atwater HA. Gallium Arsenide Solar Cell Absorption Enhancement Using Whispering Gallery Modes of Dielectric Nanospheres. *IEEE J Photovolt*. 2012;2(2):123-128.
12. Bunthof LAA, Bos-Coenraad J, Corbeek WHM, Vlieg E, Schermer JJ. The illumination angle dependency of CPV solar cell electrical performance. *Solar Energy*. 2017;144:166-174.
13. Singh P, Ravindra NM. Temperature dependence of solar cell performance—an analysis. *Sol Energ Mat Sol Cells*. 2012;101(Supplement C):36-45.
14. Green MA. *Solar Cells: Operating Principles, Technology and System Applications*. Sydney: University of New South Wales; 1998.
15. Ekonomov AP, Moroz VI, Moshkin BE, Gnedykh VI, Golovin YM, Crigoryev AV. Scattered UV solar radiation within the clouds of Venus. *Nature*. 1984;307(5949):345-347.
16. Moroz VI, Ekonomov AP, Moshkin BE, et al. Solar and thermal radiation in the Venus atmosphere. *Adv Space Res*. 1985;5(11):197-232.
17. Green MA, Hishikawa Y, Dunlop ED, et al. Solar cell efficiency tables (Version 53). *Prog Photovolt: Res Appl*. 2019;27(1):3-12.
18. Boca A, Warwick R, White B, Ewell R. A Data-Driven Evaluation of the Viability of Solar Arrays at Saturn. *IEEE J Photovolt*. 2017;7(4):1159-1164.
19. Tomasko MG, Doose LR, Smith PH, Odell AP. Measurements of the flux of sunlight in the atmosphere of Venus. *J Geophys Res Space Physics*. 1980;85(A13):8167-8186.
20. Welber B, Cardona M, Kim CK, Rodriguez S. Dependence of the direct energy gap of GaAs on hydrostatic pressure. *Physical Review B*. 1975;12(12):5729-5738.
21. Tuck B, Jay PR. Low-temperature diffusion of silver in InP. *J Phys D Appl Phys*. 1978;11(10):1413-1420.
22. Tuck B. *Atomic Diffusion in III-V Semiconductors*. Boca Raton: CRC Press; 1988.
23. Schroder DK, Meier DL. Solar cell contact resistance—A review. *IEEE Trans Electron Dev*. 1984;31(5):637-647.
24. Lukco D, Spry DJ, Harvey RP, et al. Chemical Analysis of Materials Exposed to Venus Temperature and Surface Atmosphere. *Earth Space Sci*. 2018;5(7):270-284.
25. Ang SS, Rowden BL, Blada JC, Mantooth HA. Packaging of High-Temperature Power Semiconductor Modules. *Electrochem Soc Trans*. 2010;27(1):909-914.
26. Johnson SR, Tiedje T. Temperature dependence of the Urbach edge in GaAs. *J Appl Phys*. 1995;78(9):5609-5613.
27. Steiner MA, Perl EE, Simon J, et al. AlGaInP/GaAs tandem solar cells for power conversion at 400°C and high concentration. *AIP Conf Proc*. 2017;1881(1):040007. https://doi.org/10.1063/1.5001429
28. Würfel U, Cuevas A, Würfel P. Charge Carrier Separation in Solar Cells. *IEEE J Photovolt*. 2015;5(1):461-469.
29. Needell DR, Ilic O, Bukowsky CR, et al. Design Criteria for Micro-Optical Tandem Luminescent Solar Concentrators. *IEEE J Photovolt*. 2018;8(6):1560-1567.

How to cite this article: Grandidier J, Kirk AP, Jahelka P, et al. Photovoltaic operation in the lower atmosphere and at the surface of Venus. *Prog Photovolt Res Appl*. 2019;1–9. https://doi.org/10.1002/pip.3214